Film Dichroism. V. Linear Dichroism Study of Acridine Dyes in Films with Emphasis on the Electronic Transitions Involved in the Long-wavelength Band of the Absorption Spectrum

Yukio MATSUOKA and Kiwamu YAMAOKA*

Faculty of Science, Hiroshima University, Higashisenda-machi, Hiroshima 730

(Received December 10, 1979)

The long-wavelength bands of the absorption spectra of 10-methylacridinium (MeAcr), Acridine Orange (AO), and Acridine Yellow (AY) in the poly(vinyl alcohol) film were investigated by the linear dichroism method. The parallel- and perpendicular-dichroic spectra of each dye were resolved into the long-axis and short-axis polarized absorption components. From these component bands the isotropic spectrum was reconstituted and the reduced dichroism spectrum was simulated by computer with a new technique which utilizes a general expression for the reduced dichroism of planar molecules with the multiple band structure. A weak absorption band (or bands) hidden in a strong one could be revealed by reproducing the observed isotropic and linear-dichroic spectra. The vibrational sub-bands of MeAcr were shown to have the average intervals of *ca.* 1.5×10^3 cm^{-1} for the short-axis polarized ^1L_a band and of *ca.* 0.7×10^3 cm^{-1} for the long-axis polarized ^1L_b band. In the visible region of the isotropic spectrum, the weak ^1L_a band of AO was clearly shown to consist of the fine structure with a regular energy separation, although it is overlapped with the intense ^1L_b band which is also composed of a vibrational structure. The same spectral feature was observed for AY. The dichroic results are discussed under considerations of (1) the overlap of the mutually orthogonal transition moments, whose angles were determined relative to the long axis of the C_{2v}-symmetric dye molecule, (2) the angle between the orientation axis and the long axis of the molecular plane, and (3) the average degree of orientation of dye molecules in the film.

The unambiguous interpretation of the optical rotatory dispersion or the circular-dichroic spectrum of an acridine dye bound to an optically active biopolymer is often hampered because of the overlap of several electronic transitions in the absorption spectrum.[1-6] Acridine may be considered as the mother compound for a large number of the acridine dyes, such as 10-methylacridinium (MeAcr), Acridine Yellow (AY), and Acridine Orange (AO). A thorough understanding of the electronic transitions of acridine should facilitate the precise assignment of the electronic transitions involved in the absorption spectra of those more complicated derivatives of acridine.

The apparent location and the polarization of two electronic transitions of acridine (*i.e.*, the ^1L_a and ^1L_b bands) have been determined from the linear dichroism in the stretched film,[7,8] the polarized fluorescence in solution,[9,10] and the absorption spectrum in polymer matrix.[11] The linearly-polarized absorption spectra of acridine and other related acridine dyes were reported in a previous paper,[8] in which the overlapping ^1L_a and ^1L_b bands were separated with a *reduction procedure*.[12] The fine structure of each electronic band was not analyzed in detail, because a general expression for the linear dichroism of planar molecules was not yet available. The results clearly showed that the 3,6-diamino- or 3,6-bis(dimethylamino)-derivatives of acridine also possess the two electronic transitions in the long-wavelength region of the absorption spectrum.[8] However, the exact wavelength position and the fine structure of the ^1L_a band could not be determined unequivocally because of the weak absorption intensity of the unmasked ^1L_a band, which was overwhelmed by the strong ^1L_b band.[8]

The objective of this paper is to draw a clear conclusion on the controversy over the electronic transitions involved in the long-wavelength region of the absorption spectra of AO and AY on the basis of the detailed spectral data of acridine and MeAcr. For this purpose, the expression for the reduced dichroism of planar molecules[13,14] was extended to cover the absorption spectrum composed of numerous overlapping transitions. With the aid of this general expression, the observed isotropic and reduced dichroic spectra were analyzed by assuming the appropriate Gaussian band shape for the individual absorption bands. Both the ^1L_a and ^1L_b bands of MeAcr, AO, and AY were clearly shown to consist of a series of vibrational sub-bands. The energy separation of the sub-bands was also estimated. The present results have finally clarified the enigmatic character of the absorption spectra of the 3,6-disubstituted acridine dyes.

Experimental

Materials. Acridine dyes used in this work were monocationic 10-methylacridinium (MeAcr), Acridine Orange (AO), and Acridine Yellow (AY),[8] each of which was assumed to be a planar molecule with the negligible out-of-plane transition in the wavelength region between 220 and 550 nm. Poly(vinyl alcohol), (PVA), was used as the film matrix. Preparations of sample and reference films were described before.[8]

Measurements and Analytical Method. Measurements of the dichroic absorption spectra of each dye and the determination of the long- and short-axis polarized absorption spectra were reported previously.[8] For a single absorption band lying in the molecular plane of a given planar molecule, the reduced dichroism ($\Delta A/A$) can be expressed as [13,14]

$$\frac{\Delta A}{A}=\frac{3}{2}\{3(2M_z-1)\cos^2\theta-(3M_z-2)\}\Phi \qquad (1)$$

where Φ is the orientation function and θ is the angle between the transition moment of the absorption band and the molecular z-axis, as defined in Fig. 1. The constant M_z is given by $M_z=\cos^2\phi_z$, where ϕ_z is the angle between the z-axis and the direction of the molecular orientation axis (*cf.* Fig. 1).

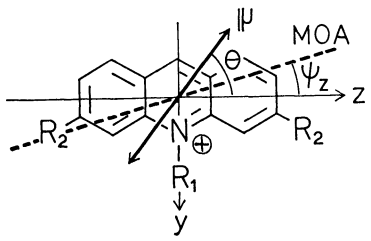

Fig. 1. Molecular coordinate system of acridine nucleus. Transition moment (μ) and molecular orientation axis (MOA) are measured from the molecular z-axis by the angles θ and ψ_z, respectively.

Equation 1 indicates that the observed quantity $\Delta A/A$ for the single absorption band should be constant over the wavelength region concerned.

If an apparent absorption band is multiple and actually consists of n component bands (i=1, n), the total reduced dichroism should be an appropriate sum from each band and may be rewritten as

$$\frac{\Delta A}{A} = \frac{\sum_{i=1}^{n}\Delta A_i}{\sum_{i=1}^{n}A_i} = \frac{\sum_{i=1}^{n}\frac{3}{2}\{3(2M_z-1)\cos^2\theta_i-(3M_z-2)\}A_i}{\sum_{i=1}^{n}A_i}\Phi \quad (2)$$

where A_i is the absorption intensity, expressed with the absorbance, of the ith band. This expression reduces to the one previously derived for the rod-like molecule which may be assumed as the unit vector (Eq. 20 in Ref. 15 where M_z=1). Equation 2 indicates that the reduced dichroism can be expressed by the quantities θ_i and A_i, which are dependent on the wavelenth λ, and by M_z and Φ, which are independent of λ and are characteristic of a particular planar molecule. The value of M_z is independent of the stretch ratio S of the film, while Φ varies with S and approaches unity as the film is stretched infinitely.[13,14] A computer simulation of an experimental reduced dichroism spectrum by the use of Eq. 2 shows the presence of weak absorption bands overlapped with strong ones.

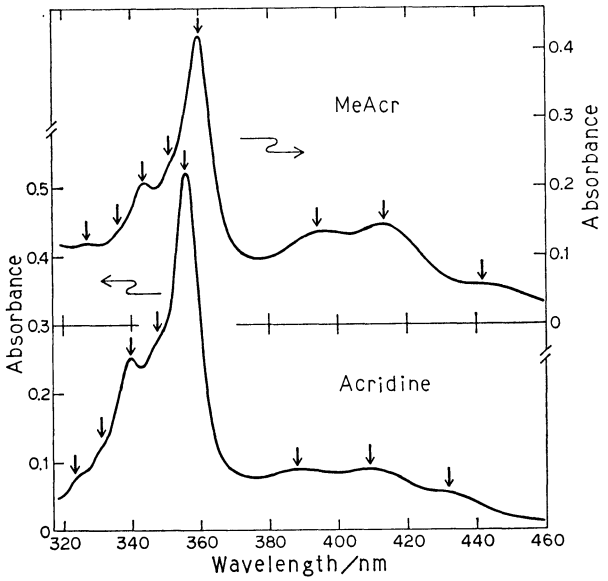

Fig. 2. Isotropic spectra of acridine and MeAcr in the nonstreched PVA film.

Results

Apparent Band Positions of Acridine and MeAcr. Figure 2 shows the isotropic spectra of acridine and MeAcr in the nonstretched (S=1) PVA film. In the spectrum of acridine, two peaks and three shoulders are observed in the 320—370 nm region and three humps in the 370—460 nm region. 10-Methylacridinium shows a similar spectrum, retaining most of these features, except for the 320—370 nm bands which are slightly diffused. From the studies of linear dichroism in the stretched polymer film[7,8] and the polarized fluorescence,[9,10] the short-wavelength band structure has been assigned to the ^1L_b transition and the long-wavelength one to the ^1L_a transition. It should be noted that the spectrum of AO differs from those in Fig. 2 in that it shows a deceptively simple absorption peak at 502 nm.[8] A similar change was always observed in the isotropic spectra of other 3,6-disubstituted acridine dyes: Proflavine, Trypaflavine, Acridine Yellow, and 10-Methyl Acridine Orange.[8] Although three shoulders are noticeable in the 400—490 nm region, the assignment of the polarization of AO was not so straightforward as in the case of acridine.[6,9,16] The isotropic spectrum of AO will be constituted from the individual component bands of the A_y- and A_z-spectra, in order to make the assignment of the polarization direction.

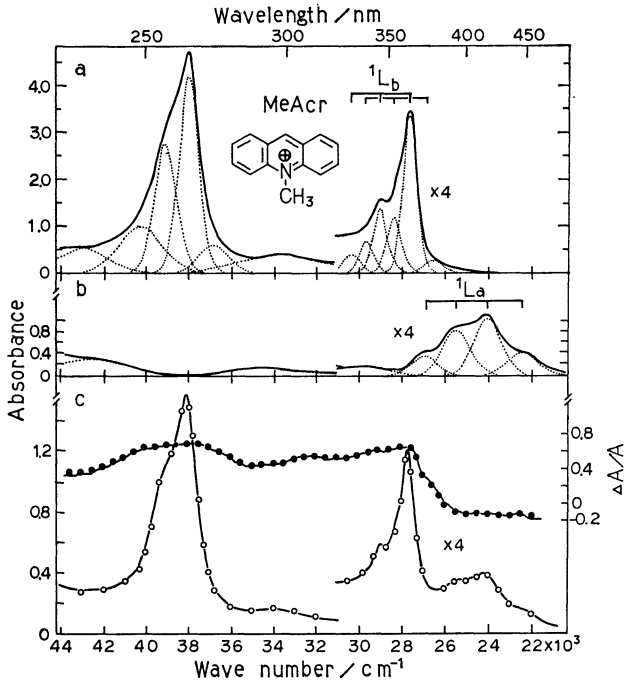

Fig. 3. Computer simulation of the dichroic data of MeAcr at Φ=0.368. (a) Resolution of the A_z-spectrum (solid curve) into the component curves (dotted). (b) Resolution of the A_y-spectrum (solid curve) into the component curves (dotted). The absorbance scale of the ^1L_b and ^1L_a bands is four-fold expanded. (c) The results of the calculated (closed circles) and experimental (solid line) reduced dichroism in the upper half, and the reconstituted (open circles) and observed (solid line) isotropic spectrum. The numerical values for the resolution are given in Table 2.

For this purpose, the dichroic spectra of MeAcr as the base data will be analyzed with Eq. 2 in some detail below.

Computer Simulation of the Isotropic and Reduced Dichroism Spectra of MeAcr. The isotropic spectrum and the long-axis and short-axis polarized spectra (*i.e.*, the A_z- and A_y-spectra) of MeAcr are shown in Fig. 3, together with the wavelength dependence of the reduced dichroism (the RD-spectrum).[8] The A_z- and A_y-spectra of MeAcr [(a) and (b) of Fig. 3] are at first divided into the respective component bands. Then, the isotropic spectrum [(c) of Fig. 3] is reconstructed from all of those component bands by a computer synthesis, in which the band envelope, $A_i(\tilde{\nu})$, of the ith component band was conventionally assumed to be the Gaussian error function at a given wave number $\tilde{\nu}$ (Eq. 3):[17,18]

$$A_i(\tilde{\nu}) = A_{i,\max} \exp\left\{-\left(\frac{\tilde{\nu}-\tilde{\nu}_{i,\max}}{\delta_i}\right)^2\right\} \qquad (3)$$

where $\tilde{\nu}_{i,\max}$, $A_{i,\max}$, and δ_i are the peak position, the maximum intensity (absorbance) at $\tilde{\nu}_{i,\max}$, and the corresponding half-width of the ith band, respectively. The half-width is the band width in wave numbers measured at 1/2.718 of the maximum height.

The resolution of the A_z-spectrum (and also the A_y-spectrum) into the component bands was carried out with a HITAC-8700 computer according to the following procedure.[15] Both $A_{i,\max}$ and δ_i were taken as adjustable parameters. Since most of the peaks and shoulders in the A_z-spectrum (and the A_y-spectrum) are easily discernible (Fig. 3), the center of each component band, $\tilde{\nu}_{i,\max}$, was treated as a pre-determined constant and was read from the respective spectra. For the sub-bands whose peak positions were not visually clear, the following guide was observed:[19] The spacing of the sub-bands is characteristic of a particular electronic transition, but each sub-band in the transition is separated more or less evenly with an average spacing $(\Delta\tilde{\nu})_{avg}$. With the pre-determined values of $\tilde{\nu}_{i,\max}$, the values of $A_{i,\max}$ and δ_i were adjusted until a reasonable agreement was obtained between the observed and simulated A_z-spectra (and A_y-spectra). This iteration procedure was repeated with a new set of $\tilde{\nu}_{i,\max}$-values in case the agreement was poor. The value of δ_i was assumed to be constant for successive sub-bands belonging to a particular electronic transition.

Figure 3 shows the resolved component bands (dotted lines) of the A_z-spectrum (a) and the A_y-spectrum (b). With the relation $3A=A_y+A_z$,[13,20] the isotropic spectrum of MeAcr can be synthesized directly by the use of those component bands. The resultant isotropic spectrum [open circles in (c)] agrees well with the observed one (solid curve). This agreement assures the correctness of the Gaussian approximation for the profile of each component band and the assumption for the spacing of the peak positions for the component bands of a particular electronic transition.

The resolution of the A_z- and A_y-spectra into the component bands is verified by the construction of the RD-spectrum. This spectrum can be simulated by using the resolved component bands with the aid of Eq. 2, in which the transition moment angles θ_i of the component bands of the A_z-spectrum are all equal to 0° and those of the component bands of the A_y-spectrum are 90° under consideration of the C_{2v} symmetry of MeAcr.[8] The values of the orientation function Φ and the constant M_z in Eq. 2 were evaluated at the same stretch ratio of 4.3 as in a previous work: $\Phi=0.368$ and $M_z=0.75$.[13] (These values may be calculated from the values of the experimental reduced dichroism with Eq. 1, if the y-axis and the z-axis polarized transitions are well separated in an absorption spectrum, as in the case of MeAcr.[14])

The result is shown in Fig. 3c, where the simulated RD-spectrum (closed circles) agrees well with the experimental one (solid curve) in the 220—460 nm region. This agreement should be considered as a strong support for the set of all A_i, θ_i, Φ, and M_z values employed in the present simulation. Thus it is obvious that the ^1L_a transition centered at 412 nm consists of four component bands with an equal spacing of *ca.* 1.5×10^3 cm^{-1}, while the ^1L_b transition centered at 360 nm consists of about six component bands with an equal spacing of *ca.* 0.7×10^3 cm^{-1}. The UV band peaked at 263 nm was resolved into four component bands. The remaining absorption region (270—340 nm) was tentatively divided into the broad component bands.

Computer Simulation of the Isotropic and Reduced Dichroism Spectra of AO and AY. In the case of AO and AY, the energy gap between the ^1L_a and ^1L_b transitions is

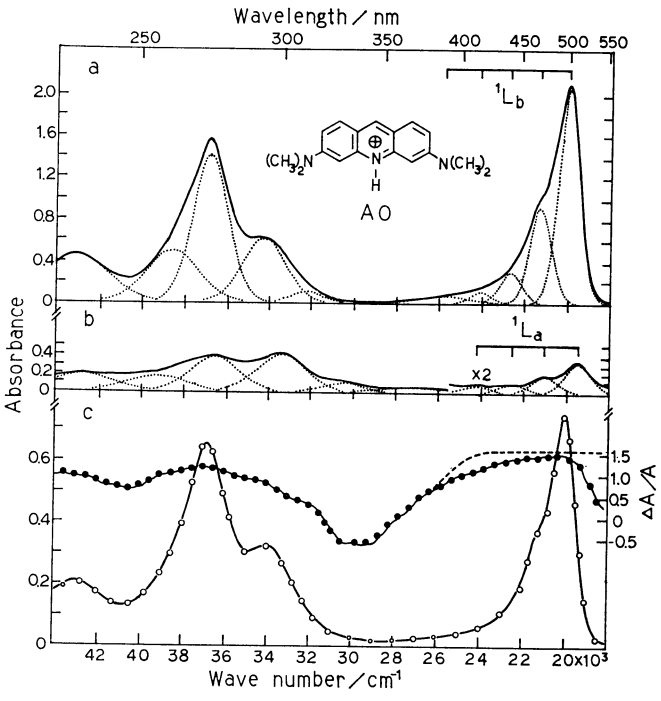

Fig. 4. Computer simulation of the dichroic data of AO at $\Phi=0.61$. Symbols are the same as in Fig. 3. The absorbance of the ^1L_a band is two-fold expanded. The thick dashed line in the visible region (c) indicates the resultant reduced dichroism under no consideration of the ^1L_a band. The presence of this band is essential to the correct reproduction of the experimental RD-spectrum.

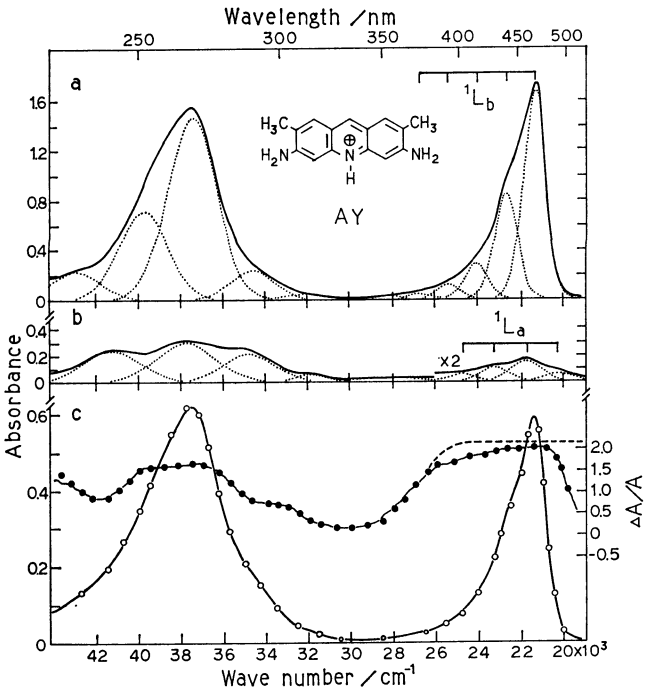

Fig. 5. Computer simulation of the dichroic data of AY at $\phi=0.72$. Symbols are the same as in Fig. 3. The absorbance of the ^1L_a band is two-fold expanded. The thick dashed line in the visible region (c) indicates the calculated reduced dichroism without the consideration of the ^1L_a band.

narrower, while the absorption intensity of the ^1L_a transition is much weaker than that of the ^1L_b transition.[8] The A_z- and A_y-spectra of AO were analyzed by the same method as used for MeAcr. The results are shown in Fig. 4, where the A_y-spectrum (b) is the average of four A_y-spectra which were obtained at four different stretch ratios. Thus the experimental error associated with the weak intensity of the A_y-spectrum was minimized. Both the A_z- and A_y-spectra of AO (a and b) were resolved into the respective component bands in the visible and UV regions. The A_z- and A_y-spectra of AY were analyzed in a manner similar to the case of AO. The results are shown in Fig. 5, which indicates that the spectral feature of AY is closely related to that of AO.

The vibrational progressions of the ^1L_a and ^1L_b bands of AY in the visible region were similar to those of AO. The A_z-spectra of AO and AY in the UV region could be divided into five component bands.[21] The highest-intensity bands at 272 nm for AO and at 266 nm for AY belong to ^1B_b transition.[9,16] However, the assignments of other bands were difficult to make. They may be either the vibrational sub-bands of the ^1B_b transition or other electronic transitions. The A_y-spectra of AO and AY in the UV region were resolved into the individual component bands. The assignments of these bands were also difficult to make. The isotropic spectra of AO and AY are finally reconstructed from those resolved bands as shown by open circles, which agree well with the observed spectra (solid curves), in Figs. 4c and 5c. The resolution of the A_z- and A_y-spectra into those component bands will be further justified by simulating the observed RD-spectrum.

The values of ϕ and M_z necessary for the simulation have already been evaluated:[13] $\phi=0.61$ (at $S=4.3$) and $M_z=0.90$ for AO, and $\phi=0.72$ (at $S=4.3$) and $M_z=1.0$ for AY. The transition moment angle θ_i is 0° for the component bands of the A_z-spectrum and 90° for the component bands of the A_y-spectrum under consideration of the molecular symmetry. The results of the simulation of the RD-spectrum are shown by closed circles for AO in Fig. 4c and for AY in Fig. 5c. The agreement between the simulated (closed circles) and the experimental (solid curve) RD-spectra is excellent over an entire wavelength region for AO and AY, which is a strong justification of both the procedure for the resolution of the A_z- and A_y-spectra into the component bands and the values of ϕ and M_z used in the simulation.

Discussion

Transition Moment Direction of an Overlapping Band and Expressions for Reduced Dichroism. If the y- and z-axis polarized electronic transitions of a molecule are isolated in the spectrum, the angle θ between either transition moment and the molecular z-axis can be determined with the aid of Eq. 1, together with the given values of M_z and ϕ. Hence, this equation yields a value of 0° for a z-axis polarized absorption band at 263 nm and 90° for a y-axis polarized band at 412 nm of MeAcr, in which these orthogonal bands are widely separated (Fig. 3). However, this is not true for the case in which two or more electronic bands are overlapped. Equation 1 is written for AO ($M_z=0.90$ and $\phi=0.61$) as

$$\frac{\Delta A}{A} = 0.915(2.4\cos^2\theta - 0.7). \quad (4)$$

This equation yields the apparent θ-values of *ca.* 25° and 82°, which differ from 0° or 90°, for the overlapping 272 nm ($\Delta A/A=1.15$) and 330 nm ($\Delta A/A=-0.60$) bands respectively (Fig. 4). Other examples are given for the representative bands of MeAcr, AO, and AY in Table 1. Molecular orbital calculations[7,22,23] prescribe that the transition moment vector of an absorption band of the acridine dyes, which belong to the C_{2v} point symmetry group, should be polarized along the long- or short-axis in the molecular plane. Accordingly, the angle θ for the overlapping bands gives only the apparent direction of a resultant vector

Table 1. The angle of transition moment, θ_λ, for some apparent bands of MeAcr, AO, and AY calculated from Eq. 1

Dyes	θ_λ[a]		
MeAcr	$\theta_{412}=90\pm3$	$\theta_{360}=12\pm3$	$\theta_{263}=0\pm3$
AO	$\theta_{502}=13\pm2$	$\theta_{330}=82\pm3$	$\theta_{272}=25\pm2$
AY	$\theta_{467}=9\pm2$	$\theta_{295}=41\pm3$	$\theta_{266}=22\pm2$

a) θ_λ is the angle in degrees measured from the z-axis of the acridine nucleus (Fig. 1), and λ in nm indicates the observed apparent band position.

Table 2. Classification on the long-wavelength absorption bands of MeAcr, AO, and AY in the PVA film

Dyes	Bands							
	^1L_a				^1L_b			
	$A_{i,max}$	δ_i	$\tilde{\nu}_{i,max}$	$\Delta\tilde{\nu}$	$A_{i,max}$	δ_i	$\tilde{\nu}_{i,max}$	$\Delta\tilde{\nu}$
		10^3 cm^{-1}	10^3 cm^{-1}	10^3 cm^{-1}		10^3 cm^{-1}	10^3 cm^{-1}	10^3 cm^{-1}
MeAcr	0.106	0.85	22.50	1.54				
	0.255	0.85	24.04	1.47				
	0.202	0.85	25.51	1.44				
	0.086	0.85	26.95		0.068	0.46	26.90	0.75
					0.827	0.46	27.65	0.72
					0.284	0.46	28.37	0.65
					0.322	0.46	29.02	0.66
					0.169	0.46	29.68	0.71
					0.096	0.46	30.39	
AO	0.157	0.85	19.50	1.60				
	0.095	0.85	21.10	1.55	2.053	0.72	19.97	1.33
	0.049	0.85	22.65	1.54	0.925	0.72	21.30	1.37
	0.035	0.85	24.19		0.305	0.72	22.67	1.37
					0.102	0.72	24.04	
AY	0.031	1.05	20.35	1.44				
	0.075	1.05	21.79	1.47	1.667	0.75	21.41	1.32
	0.054	1.05	23.26	1.49	0.842	0.75	22.73	1.35
	0.029	1.05	24.75		0.283	0.75	24.08	1.33
					0.116	0.75	25.41	1.30
					0.035	0.75	26.71	

of some differently polarized transitions. Neglect of this fact may cause some confusion in the assignment of the direction of transition moments.

The above difficulty may be avoided by the use of Eq. 2, which is written for AO as

$$\frac{\Delta A}{A} = 0.915\left(2.4\frac{A_y\cos^2\theta_y + A_z\cos^2\theta_z}{A_y + A_z} - 0.7\right). \quad (5)$$

In this equation the correct angles of transition moments, θ_y and θ_z, can be calculated to be 90° and 0° at any wavelength, provided that both A_y- and A_z-spectra are available from the reduction procedure, together with the values of M_z and Φ. It should be emphasized here that Eq. 2 is the general expression which describes the dichroic property of any planar, light-absorbing molecules with no out-of-plane transition and will be employed for the analysis of the observed $A_{//}$- and $A_{\perp}$-spectra, each of which contains some overlapping bands. In order to utilize Eq. 2 fully, the values of M_z, Φ, and $A_i(=A_y$ or $A_z)$ must be available without recourse to the reduction procedure. Both M_z and Φ may be estimated experimentally by measuring the reduced dichroism at several stretch ratios, while A_i may be obtained by equating θ_y and θ_z to 90° and 0° in Eq. 5 (or 2) for the C_{2v}-symmetric molecules.

Identification of the ^1L_a and ^1L_b Transitions of MeAcr, AO, and AY. The spectral profile of the short-axis polarized transition (^1L_a) of MeAcr could be resolved into a series of the vibrational sub-bands. The energy separation $\Delta\tilde{\nu}$ of the successive sub-bands is (1.4—1.5) × 10^3 cm^{-1} (Table 2). This spacing is very close to the previously reported values for the ^1L_a transitions of acridine[7] and some polyacenes.[24,25] The spacing of the vibrational sub-bands of the ^1L_b transition of MeAcr is (0.7—0.8) × 10^3 cm^{-1} (Table 2), as obtained from the resolution of the long-axis polarized spectrum. This energy separation is also very close to the values for the vibrational sub-bands of the ^1L_b transition of the polyacene derivatives.[25] The band profiles of the individual vibrational sub-bands associated with the electronic ^1L_b transition strongly support the notions that two different vibrational progressions are involved and that their average energy spacings are both about 1.4×10^3 cm^{-1}, as indicated in Fig. 3a. It is interesting to note that the intense, solitary peak at 360 nm is actually the second of the vibrational sub-bands. If it were the first, the RD-spectrum in Fig. 3c should ascend much more sharply from −0.2 to 0.7 in the 360—380 nm region.

From Figs, 4 and 5, it is obvious that the ^1L_a transition of AO (and AY) also consists of several vibrational sub-bands which are overlapped by the intense ^1L_b transition. If the vibrational structure were due to an error in the trial-and-error reduction search,[8,12] there would be no short-axis polarized transition (^1L_a) involved in the visible region. In this case, the calculated wavelength dependence of the reduced dichroism should differ from the experimental curve, behaving like the curve of thick dashed lines in Figs. 4c and 5c, and, hence, the experimental reduced dichroism could never be reproduced. Therefore, the short-axis polarized band must be present in the visible region of AO (and AY). The spacing of the sub-bands of the ^1L_a transition of AO (and AY) is (1.4—1.6) × 10^3 cm^{-1} (*cf.* Table 2 and Figs. 4b and 5b). This energy separation is again in good agreement with the values

for the ^1L_a transitions of MeAcr and other aromatic compounds.[25] The vibrational spacing of the ^1L_b transition of AO (and AY) is $(1.3—1.4)\times10^3$ cm^{-1} (*cf.* Table 2 and Figs. 4a and 5a) and agrees with a reported value of 1.3×10^3 cm^{-1}.[26] It is now clear from the present work why the experimental verification of the ^1L_a transition for the 3,6-disubstituted acridine dyes has long been unsuccessful. It is because the ^1L_a band is weak and completely hidden by the intense ^1L_b band.

The ^1L_a and ^1L_b bands of AO and AY are distributed over a wide wavelength region. This wide progression of the ^1L_a band of AO (and AY) may be responsible for a variety of reports on the different wavelength positions of the ^1L_a band, *i.e.*, the short-wavelength side of the principal peak (Ballard *et al.*[16] and Ito and I'Haya[23]) or the long-wavelength side of the principal peak (Wittwer *et al.*[9] and Lang and Löber[22]). The classification of the long-wavelength absorption bands of MeAcr, AO, and AY has now been completed in this work. With this result, optical studies of the interaction between acridine dyes and natural or synthetic polymers should be facilitated. The geometrical studies of the complexes between 10-Methyl Acridine Orange and deoxyribonucleic acid and sodium polyphosphate will be reported shortly.

Conclusion

The isotropic spectra of MeAcr, AO, and AY were reconstituted from the component bands obtained by resolving the long- and short-axis polarized absorption spectra (A_y and A_z). The existence of a weak absorption band (the ^1L_a band) of AO and AY could be confirmed by reproducing the experimental reduced dichroism reasonably well with the aid of a new expression for the reduced dichroism of the multiple band system. The weak ^1L_a band of both AO and AY was shown to consist of the vibrational structure with regular energy intervals. The average spacing of the successive subbands for the ^1L_a and ^1L_b transitions of MeAcr, AO, and AY could be estimated from the resolved peak positions. The general expression for the reduced dichroism of a planar molecule (Eq. 2) has proved to be useful for analyzing the linear dichroism with overlapping absorption bands in the dichroic spectra of acridine dyes of C_{2v} point symmetry.

References

1) K. Yamaoka, *Biopolymers*, **11**, 2537 (1972).
2) K. Yamaoka and S. Noji, *Chem. Lett.*, **1979**, 1123.
3) M. Zama and S. Ichimura, *Biopolymers*, **9**, 53 (1970).
4) S. Ikeda and T. Imae, *Biopolymers*, **10**, 1743 (1971).
5) E. Fredericq and C. Houssier, *Biopolymers*, **11**, 2281 (1972).
6) A. Gafni, J. Schlessinger, and I. Z. Steinberg, *Israel J. Chem.*, **11**, 423 (1973).
7) J. Yoshino, T. Hoshi, T. Masamoto, H. Inoue, and K. Ota, *Nippon Kagaku Kaishi*, **1972**, 2227.
8) Y. Matsuoka and K. Yamaoka, *Bull. Chem. Soc. Jpn.*, **52**, 3163 (1979).
9) A. Wittwer and V. Zanker, *Z. Phys. Chem. (Frankfurt am Main)*, **22**, 417 (1959).
10) W. Seiffert, H. H. Limbach, V. Zanker, and H. Mantsch, *Histochemie*, **23**, 220 (1970).
11) E. H. Park, A. H. Kadhim, and H. W. Offen, *Photochem. Photobiol.*, **8**, 261 (1968).
12) E. W. Thulstrup, J. Michl, and J. H. Eggers, *J. Phys. Chem.*, **74**, 3868 (1970).
13) Y. Matsuoka, *J. Phys. Chem.*, **84**, 1361 (1980).
14) This was presented at the annual Meetings of Molecular Structures (Bunshikozosogotoronkai) of the Chemical Society of Japan held at Tokyo in October, 1979, Abstr. p. 540, and at Hiroshima in October, 1978, Abstr. p. 590.
15) K. Yamaoka and Y. Matsuoka, *J. Sci. Hiroshima Univ., Ser. A*, **40**, 105 (1976).
16) R. E. Ballard, A. J. McCaffery, and S. F. Mason, *Biopolymers*, **4**, 97 (1966).
17) L. M. Schwartz, *Anal. Chem.*, **43**, 1336 (1971).
18) T. Nakamura and Y. J. I'Haya, *Bull. Chem. Soc. Jpn.*, **45**, 2720 (1972).
19) H. H. Jaffé and M. Orchin, "Theory and Applications of Ultraviolet Spectroscopy," John Willey and Sons, Inc., New York, N. Y. (1966), pp. 302—303.
20) B. Nordén, G. Lindblom, and I. Jonáš, *J. Phys. Chem.*, **81**, 2086 (1977).
21) H. Jakobi and H. Kuhn, *Z. Elektrochem.*, **66**, 46 (1962).
22) H. Lang and G. Löber, *Tetrahedron Lett.*, **46**, 4043 (1969).
23) H. Ito and Y. J. I'Haya, *Int. J. Quantum Chem.*, **2**, 5 (1968).
24) H. Inoue, T. Hoshi, T. Masamoto, J. Shiraishi, and Y. Tanizaki, *Ber. Bunsenges. Phys. Chem.*, **75**, 441 (1971).
25) N. D. Coggeshall and A. Pozefsky, *J. Chem. Phys.*, **19**, 980 (1951).
26) T. Kurucsev and U. P. Strauss, *J. Phys. Chem.*, **74**, 3081 (1970).